IEEE Access
Multidisciplinary ⋮ Rapid Review ⋮ Open Access Journal

Received December 22, 2020, accepted January 7, 2021, date of publication January 21, 2021, date of current version February 2, 2021.

Digital Object Identifier 10.1109/ACCESS.2021.3053310

Global and Transient Effects of Intermittent Hypoxia on Heart Rate Variability Markers: Evaluation Using an Obstructive Sleep Apnea Model

DANIEL ROMERO[1] AND RAIMON JANÉ[1,2,3], (Senior Member, IEEE)

[1]Institute for Bioengineering of Catalonia, IBEC-BIST, 08028 Barcelona, Spain
[2]Department of Automatic Control, Universitat Politècnica de Catalunya - BarcelonaTech (UPC), 08028 Barcelona, Spain
[3]Centro de Investigación Biomédica en Red de Bioingeniería, Biomateriales y Nanomedicina (CIBER-BBN), 28029 Madrid, Spain

Corresponding author: Daniel Romero (dromero@ibecbarcelona.eu)

This work was supported in part by the European Union's Horizon 2020 research and innovation programme under the Marie Sklodowska-Curie Grant 846636, in part by the CERCA Program/Generalitat de Catalunya, in part by the Secretaria d'Universitats i Recerca de la Generalitat de Catalunya under Grant GRC 2017 SGR 01770, and in part by the Spanish Grant RTI2018-098472-B-I00 (MCIU/AEI/FEDER, UE).

ABSTRACT Intermittent hypoxia (IH) produces autonomic dysfunction that promotes the development of arrhythmia and hypertension in patients with obstructive sleep apnea (OSA). This paper investigated different heart rate variability (HRV) indices in the context of IH using a rat model for OSA. Linear and non-linear HRV parameters were assessed from ultra-short (15-s segments) and short-term (5 min) analyses of heartbeat time-series. Transient changes observed from pre-apnea segments to hypoxia episodes were evaluated, besides the relative and global impact of IH, as a function of its severity. Results showed an overall increase in ultra-short HRV markers as immediate response to hypoxia: standard deviation of normal RR intervals, SDNN = 1.2 ms (IQR: 1.1-2.1) vs 1.4 ms (IQR: 1.2-2.2), p = 0.015; root mean square of the successive differences, RMSSD = 1.7 ms (IQR: 1.5-2.2) vs 1.9 ms (IQR: 1.6-2.4), p = 0.031. The power in the very low frequency (VLF) band also showed a significant increase: 0.09 ms^2 (IQR: 0.05-0.20) vs 0.16 ms^2 (IQR: 0.12-0.23), p = 0.016, probably associated with the potentiation of the carotid body chemo-sensory response to hypoxia. Moreover, a clear link between severity of IH and short-term HRV measures was found in VLF and LF power, besides their progressive increase seen throughout the experiment after each apnea sequence. However, only those markers quantifying fragmentation levels in RR series were significantly affected when the experiment ended, as compared to baseline measures: percentage of inflection points, PIP = 49% (IQR: 45-51) vs 53% (IQR: 47-53), p = 0.031; percentage of short (≥3 RR intervals) accelerated/decelerated segments, PSS = 75% (IQR: 51-81) vs 87% (IQR: 51-90), p = 0.046. These findings suggest a significant deterioration of cardiac rhythm with a more erratic behavior beyond the normal sinus arrhythmia, that may lead to a future cardiac condition.

INDEX TERMS Intermittent hypoxia, heart rate variability, obstructive apneas, hypoxia rat model.

I. INTRODUCTION

Obstructive sleep apnea (OSA) is a chronic health condition characterized by repeated apnea episodes during patients's sleep, resulting in sustained exposure to intermittent hypoxia (IH), large negative intrathoracic pressure, and arousals. This chronic condition has been extensively associated with several cardiovascular consequences, such as systemic hypertension, heart failure, coronary artery disease, arrhythmias and stroke [1]–[4]. Although the underlying mechanisms linking IH to cardiovascular diseases in OSA patients remain unclear, it has been suggested that an elevated sympathetic tone of the autonomic nervous system (ANS) [5], oxidative

The associate editor coordinating the review of this manuscript and approving it for publication was Wei Wang.

stress and endothelial dysfunction [2], [6], inflammation, and atherosclerosis [3], [7] may be contributing factors.

A large number of research studies made use of human and experimental OSA models of chronic intermittent hypoxia (CIH), to link OSA to cardiovascular diseases. In particular, animal models make possible to partially reproduce the pathological conditions whose replication in humans is restricted for safety reasons. In the context of sleep apnea, mice and especially rat models are most commonly used in experiments conducted to understand the physiological mechanisms involved in the disease. However, the protocols implemented to induce IH can differ greatly from study to study, and range from subjecting the animals to intermittent exposure of hypobaric hypoxia (by reducing FiO_2 %) to simulate altitude using static and dynamic hypoxic environments [8], to directly obstructing the animals' airways to induce hypoxic episodes such as those in OSA patients [9], [11]. This may affect the respiratory, cardiovascular, and nervous systems in different ways, leading to therapeutic and/or pathogenic effects. The characteristics of IH protocol, including the severity and duration of the hypoxic episodes, the number of episodes/day and the repetitive pattern over time are crucial for understanding the final impact of IH. Typically, chronic IH tends to be pathogenic, whereas modest exposures to IH (i.e., 9–16% inspired O_2 and few episodes) are more likely to produce beneficial effects without pathology [12].

Although in many experiments that make use of rats the animals are conscious, in many others, they are anesthetized. In such cases, cardiovascular functioning can be affected, and the control performed by the autonomic nervous system (ANS) may be partially blocked. Other factors such as the dose, type, and method used during anesthetic administration may also disrupt the control system in different ways [38]. Nonetheless, a recent study was able to report alterations in sympathetic nerve activity, sympathetic peripheral chemoreflex sensitivity and central sympathetic respiratory coupling after IH in anesthetized rats [14].

To assess the effects induced by hypoxia on cardiac signals, a rat model for recurrent apnea, simulated through periodic airway obstruction, was used [9]. The model was implemented using an external control device that varied the frequency and duration of the induced apnea episodes. Different sensors including flow and pressure transducers, skin electrodes and a pulse oximeter allowed continuous monitoring of cardiac and respiratory activity throughout the experiment. In previous work using the same model, the effects of the anesthesia were assessed through PPG signal analysis [9]. In that study, no relevant changes for heart rate variability (HRV) spectral parameters were observed during hypoxia. More recently, the overall effect on cardiac rhythm caused by IH was investigated using non-linear HRV markers [15], but limited to comparing pre- and post-IH measures.

In the present study, we aimed at evaluating the transient response of the autonomic control to hypoxia, besides the cumulative impact to cardiac functioning of IH, simulated by controlled sequences of recurrent apnea. To achieve these goals, the ANS activity was assessed by ultra-short and short-term HRV analysis using ECG instead of PPG signals, applied during hypoxic episodes and during basal segments of normal respiration, respectively. Basal segments were extracted at the beginning and end of the experiment, but also between sequences of recurrent apnea of different severity.

II. MATERIALS AND METHODS

A. POPULATION DATA

Six male and healthy Sprague-Dawley rats (mean weight: 437±27 g) were intraperitoneally anesthetized with urethane (1g/1kg). The rats were connected to a system that controls a nasal mask with one tube open to the atmosphere and another connected to a positive pressure pump, thus preventing the animal from rebreathing. OSA episodes were simulated by obstructing the airways in the tubes using electrovalves controlled by BIOPAC Systems® (CA, USA) equipment and its associated software. The electrodes, nasal mask and SpO_2 sensor were placed on the rats after the animals had been anesthetized and shaved (Fig. 1). The experimental design regarding the model was approved by the Institutional Animal Care and Ethics Committee of the Hospital Clínic, Barcelona. All the experiments were performed in accordance with the European Community Directive (2010/63/UE) and Spanish guidelines (RD 53/2013) for the use of experimental animals. Several physiological signals were acquired during spontaneous breathing and simulated OSA episodes. Respiratory flow signal, respiratory pressure and electrocardiogram (ECG) signals (leads I and II) were registered using the BIOPAC System. The photoplethysmography (PPG) signal and SpO_2 were measured by a MouseOx Plus® pulse oximeter (STARR Life Sciences Corp, PA, USA) positioned on the leg of the rats [9].

B. EXPERIMENTAL OSA MODEL

Two consecutive protocols were conducted during the experiment [9]. In both cases, recurrent apnea sequences were induced for 15-min intervals, preceded and followed by 15-min periods of normal breathing (see Fig. 1-b). Apnea index (AI) of 20, 40, and 60 events/hour were used in the first protocol (P1) [10], while the duration of the apnea episodes was 15 s (Fig. 2-a). In the second protocol (P2), the AI was fixed to 60 events/hour and the episodes lasted 5, 10, or 15 s in each sequence [11]. The order of the apnea sequences as a function of AI or apnea duration was randomly fixed alongside the experiment. However, the number of sequences with the same AI or with the same duration, was evenly distributed within the population (two rats for each case) as it is shown in Fig. 2. Both protocols were set to investigate to what extent the AI or the duration of the apnea episodes, affect HRV markers. In that sense, rats had previously been anesthetized to acquire signals at rest and to obtain suitable ECG records for analysis.

The different duration of 15, 10 and 5 s used for mechanical airway obstructions, were selected because these might result

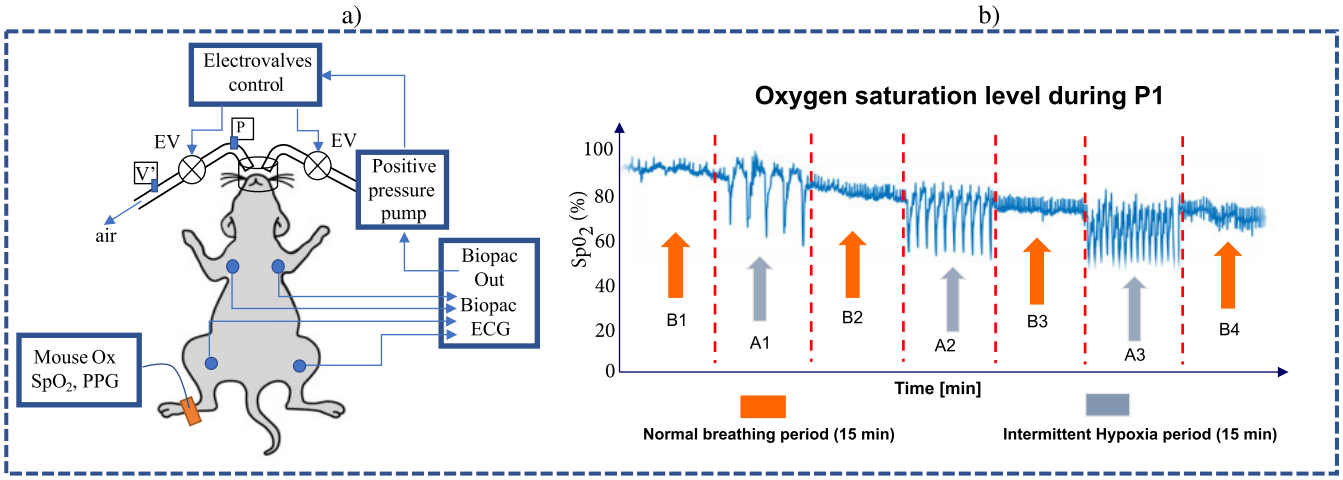

FIGURE 1. (a) Experimental setup of the rat model for OSA. Two electrovalves (EV) and a positive pressure pump were used. Signals acquired: respiratory flow (V') and pressure (P), arterial oxygen saturation (SpO_2); photoplethysmography (PPG) from Mouse Ox Plus® and two ECG leads from BIOPAC system®. b) Time-course of the SpO_2 signal during protocol P1. B1, B2, B3 and B4 indicate basal periods of normal respiration. A1, A2 and A3 represent periods of apnea sequences.

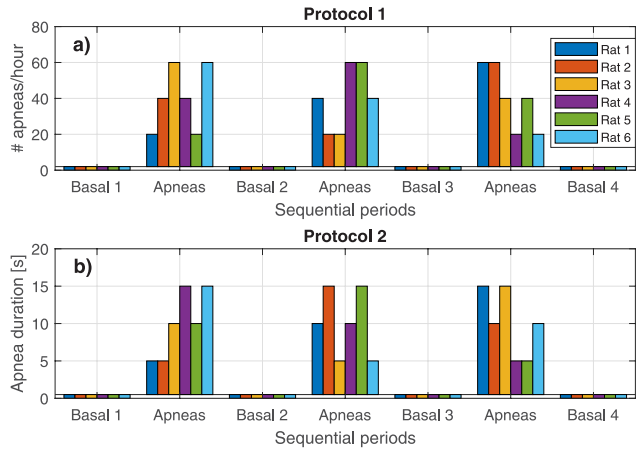

FIGURE 2. a) Protocol 1 (P1): Recurrent apnea sequences of 15-s duration episodes simulated during 15-min intervals, preceded and followed by 15-min periods of normal respiration. b) Protocol 2 (P2): Recurrent apnea sequences of 5, 10 or 15-s duration, all them simulated at 60 events/hour during 15-min intervals, preceded and followed by 15-min periods of normal respiration.

in transient SpO_2 drops to 75±2%, 83±2% and 85±1%, respectively [11]. In our database, relative drops in oxygen saturation during apnea episodes varied between 5% and 23% among all rats.

C. ECG PREPROCESSING

Raw ECG signals sampled at 1250 Hz were preprocessed before the automatic extraction of the evaluated markers. This included ECG resampling at 10 kHz, baseline drift attenuation via cubic spline interpolation [16], 4^{th} order bidirectional Butterworth low-pass filtering at 45 Hz to retain main QRS components by removing power-line interference and high-frequency noise and finally, automatic QRS complex detection [17] followed by a visual inspection to exclude noisy beats in noisy ECG segments. The resampling step was performed to improve time resolution for R peak detection [18], considering that the heart rate range in rats is significantly faster than in humans (around 300-500 bpm). The final location of the R peaks was determined from the non-filtered ECG based on detected QRS complexes, and used to generate the RR time-series analyzed in the study.

D. HEART RATE VARIABILITY ANALYSIS

The analysis of the HRV included linear and non-linear methods to characterize different stages and phases of the designed protocol. Three analyses were performed: a) an ultra-short term analysis to evaluate the transient response to apnea events; b) the impact of IH severity as a function of AI values; c) the cumulative effects of IH over the course of the experiment. In the first analysis, markers were evaluated in short segments of 15 s, taken before the onset and during each apnea episode. In the two remaining analyses, markers were evaluated in selected segments of 5-min duration (short-term analysis). Moreover, a) and b) were performed only for protocol P1 because of its different AI values, while the analysis in c) included both the P1 and P2 protocols.

1) TEMPORAL-DOMAIN ANALYSIS

From the RR time-series, we obtained temporal parameters such as the standard deviation of normal RR intervals (SDNN), the root mean squares of the successive differences of NN intervals (rMSSD), and the percentage of differences between adjacent NN intervals greater than x ms (pNNx, %). In human studies, the value of x is typically set to 50 ms to distinguish between physiological and pathological conditions. To adapt this parameter to the rats, we tested different values of x (6, 8 and 10 ms) according to their normal range of RR intervals [19]. All markers were considered in the three analyses previously mentioned.

2) FREQUENCY-DOMAIN ANALYSIS

The spectral parameters were obtained using two different approaches depending on the segment length. The first one used the power spectral densities (PSD) estimated by Welch's method using a Hanning window. Before estimating the PSD, the RR interval time-series were interpolated at 15 Hz using the cubic spline approach to make the time-series evenly sampled. Next, these series were analyzed using half-overlapping segments of 512 samples. Hanning windowing is intended to attenuate side effects which lead to spectral leakage. Finally, the PSDs were integrated within the three bands described below to obtain the spectral markers. This approach was only used for those analysis involving 5-min segment length.

The oscillatory components of the ANS calculated from the PSD were defined as follows: the very low frequency band (VLF: 0.01 to 0.20 Hz), the low frequency band (LF: 0.20 to 0.75 Hz) and the high frequency band (HF: 0.75 to 2.50 Hz) expressed in ms^2 [19]–[21]. The normalized versions of these markers (VLF_{no}, LF_{no} and HF_{no}) were also computed in relation to the total power, obtained as the sum of the three components. The ratio LF/HF was computed from the normalized components, but considering the total power as the sum of LF and HF in this case.

In the second approach, aimed for the ultra-short-term analysis, we used the smoothed pseudo-Wigner-Ville distribution (SPWVD) to obtain the time-frequency maps from which the spectral markers were estimated. Because the classic spectral analysis requires stationary data to estimate the ANS modulation accurately, and because the signals in the experiment may be non-stationary, spectral characteristics must be analyzed using a time-frequency (TF) approach to track temporal variations. Indeed, spectral markers derived from SPWVD have been evaluated in clinical and experimental studies, demonstrating a strong correlation with traditional HRV spectral markers [22], [23]. The Wigner-Ville distribution (VWD) is a quadratic time-frequency method defined as the Fourier transform of the instantaneous autocorrelation function [24]. Since WVD is affected by significant interference terms, a smoothing kernel function $\Psi(\tau, \upsilon)$ is introduced to attenuate these interferences while maintaining a suitable time-frequency resolution, with τ and υ representing the domain variables of time and frequency lags, respectively [25]. Being $A_{RR}(\tau, \upsilon)$ the Ambiguity Function of the RR time series, $x_{RR}(t)$, the SPWVD is defined as:

$$A_{RR}(\tau, \upsilon) = \int_{-\infty}^{\infty} x_{RR}(t + \frac{\tau}{2}) x^*_{RR}(t - \frac{\tau}{2}) e^{-j2\pi\upsilon t} dt \quad (1)$$

$$\Psi(\tau, \upsilon) = \exp\left\{-\pi\left[\left(\frac{\upsilon}{\upsilon_0}\right)^2 + \left(\frac{\tau}{\tau_0}\right)^2\right]^{2\lambda}\right\} \quad (2)$$

$$C_{RR}(t, f) = \int\int \Psi(\tau, \upsilon) A_{RR}(\tau, \upsilon) e^{j2\pi(t\upsilon - tf)} dt d\upsilon \quad (3)$$

where t and f denote time and frequency, respectively, while λ sets the roll-off of the kernel. The parameters of the kernel function were adjusted to $\upsilon_0 = 0.06$ and $\tau_0 = 0.03$, obtaining temporal and spectral resolutions of 16.7 seconds and 0.033 Hz, respectively. This combination led to an efficient interference terms cancellation for the lowest TF filtering [26]. Then, HRV indices were measured as the total power in VLF, LF and HF bands, in specific 15-s segments from the SPWVD.

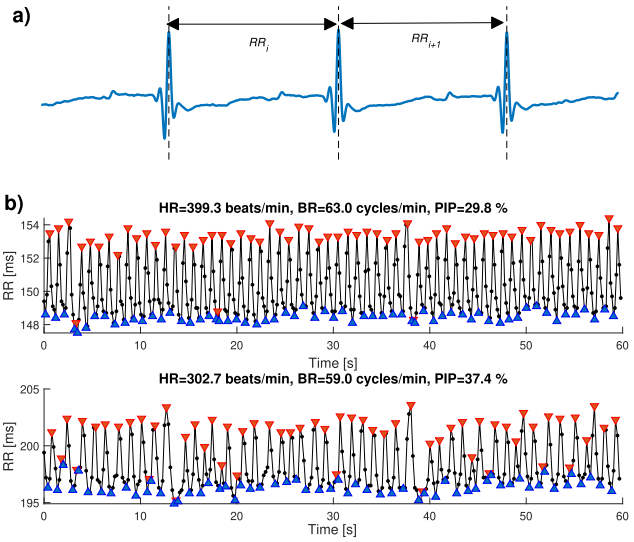

FIGURE 3. a) Representative ECG segment extracted during baseline with the associated RR intervals. b) RR interval time-series representing 60-s segments, extracted during the initial and final basal periods of the experiment. Red and blue triangles indicate inflection points detected on these segments. Heart rate (HR), respiratory rate (BR) and PIP values are displayed at the top of the graphs.

3) NON-LINEAR HRV ANALYSIS

To quantify abnormal fluctuations in the RR time-series beyond normal sinus arrhythmia (NSA), we computed a set of non-linear parameters that evaluate the level of fragmentation in the cardiac rhythm, whose increase is associated with the disruption of the neuroautonomic control system of the sinoatrial node [27]. Basically, these parameters estimate the number of changes in the heart rate acceleration sign (i.e., inflection points in RR time-series), translated into more rapid changes between acceleration and deceleration segments in the RR time-series. The parameters are defined as follows:

- PIP: represent the percentage of inflection points (IP) for a given segment of the RR time-series. This is equivalent to the number of zero-crossing points, found in the first derivative of the time series, in relation to the total segment length.
- IALS: the inverse average length of the acceleration and deceleration segments. These segments represent consecutive RR intervals between adjacent inflection points whose differences are negative or positive.
- PSS: the percentage of RR intervals in short segments, defined as the acceleration or deceleration segments that lasted ≥ 3 RR intervals.

Fig. 3 shows two segments of the RR time-series, extracted during the initial and final stages of the experiment for a

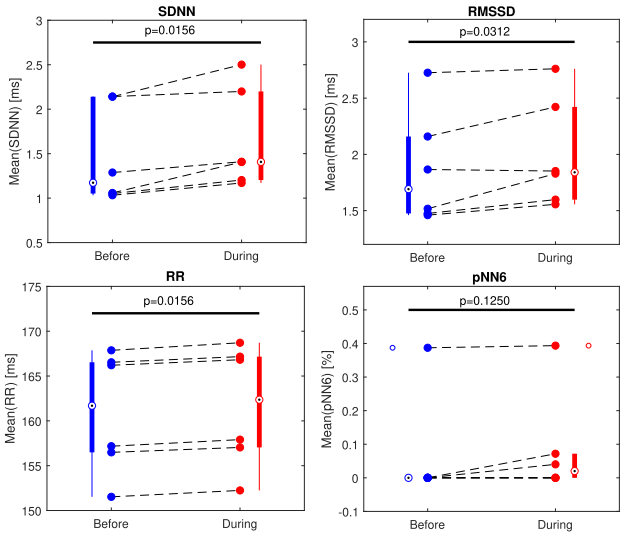

FIGURE 4. Mean values of the temporal HRV markers (*SDNN*, *RMSSD*, *RR*, *pNN6*) before and during apnea episodes evaluated during protocol P1 (30 episodes per rat). Filled circles represent individual mean values for each rat, while boxplots indicate the median and interquartile range of the group at different stages.

particular recording. It reveals that most of the IP detected were due to respiration modulation and that this modulation is less stable after IH, as observed during the final segment. Since these fragmentation parameters can be highly influenced by both the heart rate (HR) and respiratory rate (BR), their relationships during the above segments were also investigated.

E. STATISTICAL ANALYSIS

Results are expressed in median and interquartile range (IQR). Paired observations obtained at different stages of the experiment were compared using the Wilcoxon signed-rank non-parametric test. The relationship between the fragmentation HRV parameters and both HR and BR was determined using Pearson's correlation coefficient. Similarly, the effects of intermittent hypoxia considering the frequency of the apnea episodes were also assessed. The significance level was set to 0.05 in all analyses. Data were processed and analyzed using custom MATLAB routines.

III. RESULTS

A. TRANSITORY RESPONSE OF AUTONOMIC CONTROL DURING APNEA EPISODES

The results obtained for the temporal HRV markers as a result of the ultra-short-term analysis during apnea episodes are summarized in Fig. 4. The mean values were obtained using all events of the P1 protocol and for each rat, considering that their duration was the same (15 s).

As shown, the overall behavior of the markers presented indicates a transient increase in HRV before and during apnea episodes, reflected in greater *SDNN* (1.2 (IQR: 1.1-2.1) vs 1.4 (IQR: 1.2-2.2) ms, $p = 0.0156$) and *RMSSD* (1.7 (IQR: 1.5-2.2) vs 1.9 (IQR: 1.6-2.4) ms, $p = 0.0312$) values, as well

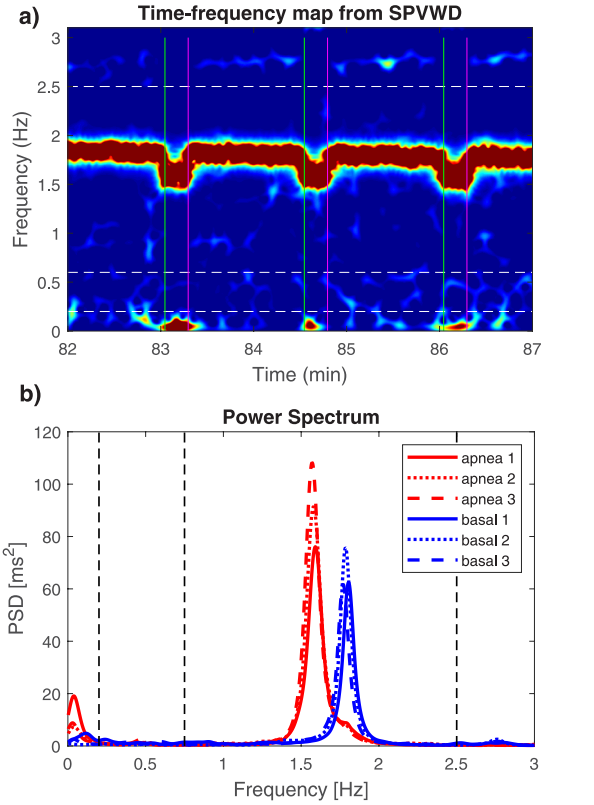

FIGURE 5. a) Time-frequency map of the RR interval time-series during three consecutive apnea episodes of 15-s duration. b) Power spectral density evaluated for 15-s segments before (in blue) and during (in red) the apnea episodes. In A), VLF, LF and HF frequency bands are delimited by the horizontal dashed lines (in white) and in B), by the dashed vertical lines (in black).

as a slight increase in the average cardiac period given by the mean *RR* values, 161 (IQR: 156-166) vs 162 (IQR: 157-167) ms, $p = 0.0156$. The *pNN6* marker was the most suitable and sensitive among the different *pNNX* variants analyzed, which also showed a slight increase during apnea episodes. However, among these markers, only *pNN6* did not change significantly from pre-apnea to obstructive segments, as confirmed by the corresponding p-value ($p = 0.1250$).

In addition, Fig. 5-a shows the time-frequency map obtained during an isolated apnea episode as well as the preceding and subsequent seconds. The PSD of these segments which are delimited by the vertical lines (15 seconds before and during the episode) are also shown. A remarkable increase in the power of the VLF band during apnea can be observed, as well as a shifting of the dominant frequency within the HF band due to respiratory effort occurring in that interval, despite airway obstruction. The transient shift of the dominant frequency is accompanied by an increase in power (see Fig. 5-b), thus affecting the total power in that band. Results of the spectral parameters were obtained only from SPVWD as illustrated in Fig. 5 for this ultra-short analysis. Table 1 summarizes the mean values for the frequency-domain markers, and the statistics obtained when comparing the pre-apneic and apneic segments. Significant increased values were found only for markers *VLF*, *LF*

TABLE 1. Average values (median and inter-quartile range (IQR)) for the spectral parameters of ultra-short-term HRV analysis evaluated before and during apnea episodes for the whole population.

Parameter	Before apnea Median (IQR)	During apnea Median (IQR)	P
VLF (ms^2)	0.09 (0.05-0.20)	0.16 (0.12-0.23)	**0.016**
LF (ms^2)	0.16 (0.07-0.60)	0.18 (0.09-0.62)	**0.016**
HF (ms^2)	2.29 (2.12-8.38)	2.98 (2.21-5.12)	0.156
TP (ms^2)	2.47 (1.89-5.90)	3.22 (2.42-8.64)	**0.016**
VLF_{no} (%)	2.19 (1.90-3.65)	3.67 (3.38-4.24)	**0.031**
LF_{no} (%)	6.28 (2.77-8.96)	5.79 (2.77-8.64)	0.578
HF_{no} (%)	90.73 (86.27-95.32)	90.40 (83.96-93.57)	0.984
LF/HF	0.07 (0.03-0.11)	0.07 (0.03 - 0.10)	0.422

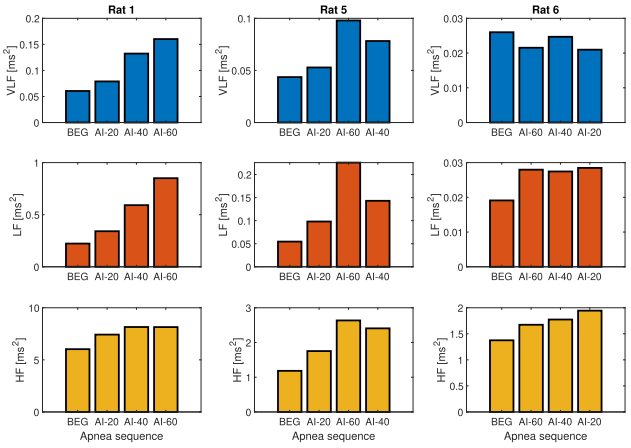

FIGURE 6. Spectral markers evaluated for three representative rats after recurrent apnea sequences with different AI values. The order of the simulated sequences was different in each animal according to the fixed AI values (20, 40 and 60 events/hour). BEG stands for basal values measured at the beginning of the experiment.

and *VLFno* assessed from the inter-recording analysis (see Table 1). Moreover, when analyzing these markers separately for each rat, we found more meaningful increases from basal segments to apnea episodes when performing the intra-recording analysis (30 episodes per rat). Table 2 summarizes the average values of *VLF* and *VLFno*, evaluated before and during apnea episodes for all rats. As the table shows, a clear increase occurred during apnea episodes, supported by their significant p-values. Except for the first rat, all of them were less than 0.001.

B. IMPACT OF APNEA SEVERITY RELATIVE TO THE NUMBER OF EVENTS AND TIME

The intra-recording effects on HRV markers as a function of apnea episodes per hour, and thus associated with IH severity, are shown for three representative examples in Fig. 6. All values used for AI in the designed protocol are represented, including 20, 40 and 60 events/hour. A clear relationship between the spectral markers and the AI values was observed for the first two examples (Rats 1 and 5), despite the random order used to simulate the apnea sequences. For Rat 1 in the left column, the markers steadily increased with the successive increase in AI. However, for the rat in the second column, the order of AI values was altered, which is reflected in the higher values of the parameters after the second sequence (AI = 60), followed by a decrease after the last sequence in the final part of the protocol, when AI was set at 40 events/hour. Finally, Rat 6 displayed a more random behavior, but nevertheless showed a time-based progressive increase in LF and HF markers regardless of AI.

Similarly, Fig. 7 (upper graphs) represents the distribution and average values of spectral markers measured at the beginning of the first protocol and after different recurrent apnea sequences, during normal respiration periods. In these cases, the AI value used in each sequence was randomly generated for each rat as described before, but the original sequential order is maintained over time. As shown, both the *VLF* and *LF* markers tend to increase over time, probably due to the cumulative effect of IH and despite the different values of AI in the apnea sequences. However, in the middle graphs, the original order of the sequences over time is no longer valid, and the average measures were pooled according to AI values. This polling showed that, even when similar sequences were simulated at different timing of the protocol, their effects on the spectral markers were in part associated with the applied AI. That is, the higher the number of events/hour, the stronger the impact on the HRV markers. Finally, in the bottom graphs the AI values associated with each measure are specified by different colors. They showed, for instance, that a value for AI equal to 60 events/hour caused more impact on the VLF and LF markers if fixed at the end of the protocol than when it was set at the beginning. Although the results in Fig. 7 show a gradual increase in the markers, the changes were not significant at least during the first protocol (P1). The remaining markers including temporal and fragmentation measures were found to be even less sensitive, regardless of the severity of IH.

C. OVERALL EFFECTS CAUSED BY THE INTERMITTENT HYPOXIA ON HRV MARKERS

Table 3 summarizes the results obtained for all markers relative to HRV analysis before and after completion of the two protocols. Unlike the previous analyses, only the total changes are considered to assess the global impact caused by the whole set of the recurrent apnea sequences provoked in each individual rat. Fragmentation markers (PIP, IALS and PSS) and mean heart period significantly changed after experiment completion. In both cases, the values of these markers increased compared to baseline measures. None of the remaining parameters varied significantly due to IH.

Fragmentation markers were correlated against the mean heart rate (in beats/min) obtained for each animal, evaluated during the initial and final stages. Results are shown in Table 4, where a strong association ($r = 0.79$) was observed after the experiment had finished compared to that found when it started. However, when the same analysis was performed against the mean BR values and the ratio given by HR/BR, stronger correlation coefficients were found in both the initial and final stages ($r \geq 0.85$). In most rats, the HR and BR parameters decreased in relation to the initial values. The

TABLE 2. Standard and normalized *VLF* parameter evaluated in each rat. Average values were obtained from all events simulated during the first protocol ($N = 30$) and computed before and during the simulated apnea episodes.

Recording	Before apnea VLF (ms^2) median (IQR)	During apnea VLF (ms^2) median (IQR)	p	Before apnea VLFno (%) median (IQR)	During apnea VLFno (%) median (IQR)	p
Rat 1	0.16 (0.13-0.28)	0.23 (0.19-0.28)	0.0321	1.76 (1.42-2.73)	1.99 (1.63-2.52)	0.3036
Rat 2	0.16 (0.10-0.25)	0.27 (0.15 - 0.37)	0.0008	1.99 (1.29-2.97)	3.19 (1.70-4.34)	0.0009
Rat 3	0.08 (0.06-0.09)	0.13 (0.09-0.16)	0.0001	3.39 (2.55-4.35)	3.94 (3.13-5.19)	0.0189
Rat 4	0.04 (0.03-0.06)	0.11 (0.09-0.13)	< 0.0001	1.56 (1.26-2.04)	3.51 (2.54-4.02)	< 0.0001
Rat 5	0.09 (0.06-0.12)	0.20 (0.12-0.23)	0.0003	4.14 (3.18-6.25)	6.76 (4.99-8.89)	0.0001
Rat 6	0.03 (0.02-0.05)	0.07 (0.05-0.10)	<0.0001	1.56 (1.19-3.03)	3.09 (2.18-3.67)	<0.0001

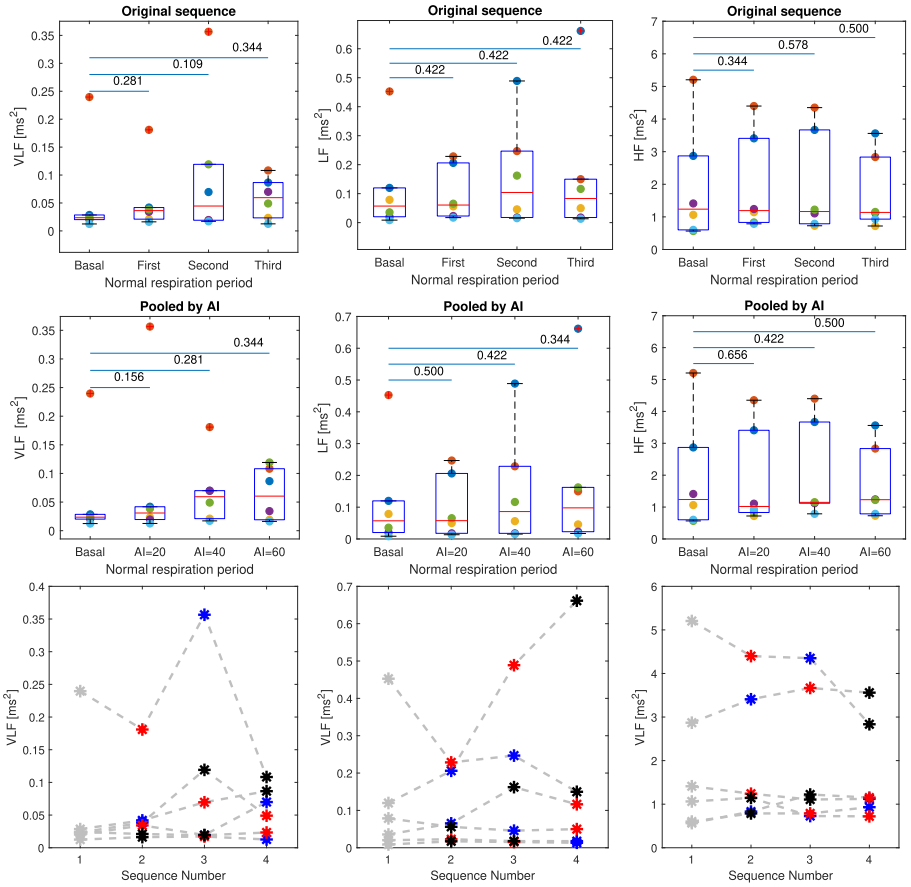

FIGURE 7. Spectral parameters computed during the initial basal period and after each sequence of recurrent apnea (periods of normal breathing). Upper graphs illustrate the values distribution over time after induced apnea sequences in their original order. Middle graphs show the values distribution after pooling them by the number of episodes/hour applied in each apnea sequence. Bottom graphs reproduce the information in the first row but showing the AI values corresponding to each measure with different colors. AI = 20 (blue), AI =4 0 (red), AI = 60 (black). Gray marks represent the baseline measures. Numbers above the horizontal lines indicate the p-values resulting from the statistical comparisons.

HR/BR ratio was also reduced at the end of the experiment, maintaining the same strong (negative) correlation with the fragmentation values. Similar results were obtained for the PSS and IALS markers as summarized in Table 4.

IV. DISCUSSION

In this study, we evaluated a set of HRV markers, including temporal and frequency domain parameters, as well as measures to estimate the level of fragmentation in heartbeat time series. We investigated how intermittent hypoxia, simulated by well-controlled sequences of recurrent apnea, can affect the cardiac functioning and the autonomic control response. Three different analyses were carried out to assess: 1) the transient effects during individual apnea episodes; 2) the relative impact of recurrent apnea sequences as a function of their severity and; 3) the overall impact of intermittent hypoxia at the end of the experiment.

Particularly, the ultra-short analysis using 15 s was motivated by the fact that in several clinical studies, segments shorter than 5 min (10, 30 and 60 s) have been explored

TABLE 3. Median and interquartile range of all HRV parameters, including temporal, spectral and fragmentation markers. Values were computed from short-term analysis (5 min) at the beginning and end of the experiment.

Parameters	Before IH	After IH	p
$SDNN$ (ms)	1.2 (1.0 – 2.4)	1.6 (1.4 – 1.8)	0.5000
$RMSSD$ (ms)	1.7 (1.2 – 3.3)	1.9 (1.7 – 2.1)	0.6562
$pNN6$	0.0 (0.0 – 0.6)	0.0 (0.0 – 0.0)	0.9999
RR (ms)	152 (148 – 163)	166 (164 – 178)	**0.0313**
VLF (ms^2) 10^{-3}	31 (28 – 51)	40 (26 – 53)	0.6562
LF (ms^2) 10^{-3}	42 (15 – 98)	87 (26 – 153)	0.5000
HF (ms^2)	1.1 (0.6 – 3.0)	1.4 (1.2 – 1.6)	0.5781
$VLFno$ (%)	2.5 (1.9 – 3.4)	1.9 (1.7 – 2.7)	0.7187
$LFno$ (%)	2.8 (2.3 – 6.5)	5.6 (1.8 – 10.0)	0.2813
$HFno$ (%)	97 (93 – 98)	94 (90 – 98)	0.7813
LF/HF 10^{-3}	29 (23 – 70)	61 (19 – 111)	0.2188
PIP (%)	49 (45 – 51)	53 (47–53)	**0.0313**
PSS (%)	75 (51 – 81)	87 (51–90)	**0.0469**
$IALS$ (%)	49 (45 – 51)	53 (48 – 53)	**0.0313**

TABLE 4. Pearson's correlation coefficients *r* obtained between the fragmentation markers of the HRV and the mean heart rate, mean respiratory rate and their ratio, HR/BR.

Fragmentation markers	$\overline{HR}$ Before | After r | r	$\overline{BR}$ Before | After r | r	$\overline{HR/BR}$ Before | After r | r
PIP (%)	-0.07 | 0.79	0.95 | 0.93	-0.99 | -0.94
PSS (%)	-0.07 | 0.72	0.94 | 0.85	-0.97 | -0.85
IALS (%)	-0.07 | 0.79	0.95 | 0.93	-0.99 | -0.93

and compared to the standard HRV analysis (5-min segments), considered as the benchmark in humans [28]. These studies concluded that some parameters obtained from ultra-short analysis remain as reliable surrogates of standard HRV parameters, especially time-domain markers such as the SDNN and RMSSD [29]. In the case of spectral markers that require a minimal segment length to be estimated, a time-frequency approach was applied so as to track possible transient changes. Compared to humans, the segment length can be shorter in rats since the frequency bands limits are shifted towards greater values, as described in section II-D2.

The results highlighted the following major findings. First, from the ultra-short-term analysis, we found a transient increase in HRV during apnea episodes, translated into higher values of *SDNN*, *RMSSD* and *RR*, in relation to pre-apneic values. Particularly, the increase in *RMSSD* may suggest parasympathetic activation when obstructive apnea episodes took place [30]. However, it might be associated with the increase in the high-frequency power caused by the animal's respiratory effort during mechanical obstruction, as illustrated in Fig. 5-b. The breathing effort somehow maintains the high-frequency oscillations, to an even greater extent than that occurring during normal respiration, as relevant changes in negative intrathoracic pressure may affect heart rate through different mechanisms [31], [32]. Moreover, absolute and normalized measures of *VLF* power estimated from the pseudo Wigner-Ville distribution also showed a significant increase during apnea events ($p = 0.016$ and $p = 0.031$, respectively), probably related to the potentiation of the carotid body's chemosensory response to hypoxia, which occurred in most episodes where SpO_2 dropped by more than 3% [33]. Although in that study chemosensory response was related to sympathetic activation measured from the LF band, other studies in OSA patients have suggested VLF power as a more reliable marker of sympathetic modulation than traditional LF/HF and LF markers, specially in patients with heart failure. Therefore, OSA seemed to be a powerful enough stimulus to produce a sympathetic discharge in the VLF range of the apnea cycle [34]. This finding was in line with the results reported in Shiomi *et al.* [35], performed with patients suffering from OSA, where increase in VLF power and the presence of a shaped VLF peak, were synchronized with episodes of respiratory arrest or hypoxemia (decreased SaO_2) that occurred at cycle lengths of 25-120 seconds. Lianj *et al.* [36] also studied the impact of mixed pathological respiratory events including hypopneas, obstructive and central sleep apneas, reporting increased VLF and LF power compared to normal respiration segments. The influence of sleep stages has also been evaluated independently for pathological respiration and in combination with cortical arousals, with the latter having the greatest impact on LF power [37]. In our study, most of the spectral parameters increased transiently during obstructive apneas, but only *VLF* and *TP* changed significantly, the latter as a result of the *VLF* increase. It was also the case for the intra-recording analysis performed over protocol P1, where *VLF* and *VLFno* significantly increased (p <0.001) in most rats (see Table 2). The major difference with respect to the aforementioned studies concerns the length of the analyzed segments and the time-frequency approach used to properly evaluate the spectral markers.

The second important finding concerns the impact of apnea severity on HRV measures evaluated during initial and subsequent basal segments of normal respiration. We considered the number of events/hour used in each sequence to assess its impact to hypoxia-induced HRV changes. Spectral markers and more specifically *VLF* and *LF* values increased over time following each sequence of intermittent hypoxia, regardless of the AI values, suggesting a cumulative hypoxia-induced effect over the course of the experiment. Furthermore, a pooled analysis of the apnea sequences showed that, despite their distinct temporal location within the experiment, changes in spectral markers were also related to AI values. Importantly, this analysis was performed only during protocol P1 where the apnea episodes presented the same duration, as opposed to those used in protocol P2, and therefore, similar drops in oxygen saturation level are expected to occur during the hypoxic episodes of the same recording. Nevertheless, the cumulative time of exposure to IH did no appear to produce and maintain significant changes after each apnea sequence, even at the end of protocol P1.

Finally, when all HRV markers were compared together, only those estimating fragmentation levels in the RR time-series were significantly affected after completion of the two protocols. Our results demonstrated that fragmentation

levels increased (between 5% and 10%, $p < 0.05$) at the end of the experiment, when all simulated sequences had been finished. In addition, we found that mean respiratory rate and its relationship to mean heart rate were highly correlated with fragmentation parameters ($|R| \geq 0.85$). This suggests that heart rate and respiratory rate could be used to obtain indirect measures of fragmentation levels, or even to adjust or normalize fragmentation estimates. For instance, in the study conducted by Costa *et al.* [27], fragmentation in RR time-series was demonstrated to increase with age in healthy subjects, as well as in patients with heart diseases such as coronary artery disease (CAD). However, fragmentation tends to be higher in patients with CAD than in healthy subjects of similar ages. They also showed that fragmentation level seems not to be affected by mean heart rate; however, our study demonstrated a strong correlation with breathing rate and the ratio HR/BR, even under different conditions. Nevertheless, our results should be interpreted with caution due to the small size of the population, and possible effects induced by anesthesia on the cardiovascular system [38].

The study was subject to some limitations, notably the small sample size that may hamper the strength of the statistic analyses. Likewise, only three categories were established when setting the frequency and duration of the apnea episodes. This fact did not allow to account for a wide range of values to represent the hypoxia severity. Moreover, although randomly, these categories were applied for each individual rat, thus limiting the estimation of the underlying relationship with the changes observed in HRV markers. One possible alternative might be performing similar analyses using polysomnographic (PSG) recordings acquired in OSA patients from larger cohorts. However, although a wide range of disease severity values may be obtained, it should be considered that in these patients apneas have varying durations and occur at non-periodic intervals. In such a case, pooling the apnea events within narrow duration ranges would be suitable to assess transient responses for different durations. Moreover, evaluating PSG recording segments with the highest obstructive event frequency, adjusted by events duration, would better to assess OSA patient's risk for a future cardiac condition.

V. CONCLUSION

Our results have shown that the HRV increases as the first transient response to hypoxia during apnea episodes. Although some markers were slightly sensitive to hypoxic episodes in the ultra-short analysis, only fragmentation measures captured significant global changes due to intermittent hypoxia. Further studies must evaluate the impact of the heart and respiratory rates on these fragmentation signatures. The number of events/hour also seems to have a relative impact on HRV markers, validating the clinical relevance of the Apnea-Hypoapnea Index (AHI) in OSA patient's prognosis. Such alterations of autonomic control, mainly driven by an increased sympathetic activity, may favors the development of cardiac arrhythmias in these patients. In the future, the application and usefulness of these markers in the assessment of OSA patients should be tested, together with the ultra-short HRV analysis adapted to the human heart's physiology.

ACKNOWLEDGMENT

The authors are grateful to Puy Ruiz, from the IBEC, and Marta Torres, Isaac Almendros, Ramon Farré and Daniel Navajas, from the Universitat de Barcelona, for their help in designing and implementing the animal model.

REFERENCES

[1] N. R. Prabhakar, "Invited review: Oxygen sensing during intermittent hypoxia: Cellular and molecular mechanisms," *J. Appl. Physiol.*, vol. 90, no. 5, pp. 1986–1994, May 2001, doi: 10.1152/jappl.2001.90.5.1986.

[2] L. Lavie, "Obstructive sleep apnoea syndrome—An oxidative stress disorder," *Sleep Med. Rev.*, vol. 7, no. 1, pp. 35–51, Feb. 2003, doi: 10.1053/smrv.2002.0261.

[3] L. Lavie, "Sleep-disordered breathing and cerebrovascular disease: A mechanistic approach," *Neurol. Clin.*, vol. 23, no. 4, pp. 1059–1075, Nov. 2005, doi: 10.1016/j.ncl.2005.05.005.

[4] E. C. Fletcher, "Invited review: Physiological consequences of intermittent hypoxia: Systemic blood pressure," *J. Appl. Physiol.*, vol. 90, no. 4, pp. 1600–1605, Apr. 2001, doi: 10.1152/jappl.2001.90.4.1600.

[5] N. R. Prabhakar and G. K. Kumar, "Mechanisms of sympathetic activation and blood pressure elevation by intermittent hypoxia," *Respiratory Physiol. Neurobiol.*, vol. 174, nos. 1–2, pp. 156–161, Nov. 2010, doi: 10.1016/j.resp.2010.08.021.

[6] M. Badran, S. Golbidi, A. Devlin, N. Ayas, and I. Laher, "Chronic intermittent hypoxia causes endothelial dysfunction in a mouse model of diet-induced obesity," *Sleep Med.*, vol. 15, no. 5, pp. 596–602, May 2014, doi: 10.1016/j.sleep.2014.01.013.

[7] J. Garvey, C. Taylor, and W. T. McNicholas, "Cardiovascular disease in obstructive sleep apnoea syndrome: The role of intermittent hypoxia and inflammation," *Eur. Respiratory J.*, vol. 33, no. 5, pp. 1195–1205, Apr. 2009, doi: 10.1183/09031936.00111208.

[8] R. K. Hetzler, C. D. Stickley, I. F. Kimura, M. W. LaBotz, A. W. Nichols, K. T. Nakasone, R. W. Sargent, and L. P. A. Burgess, "The effect of dynamic intermittent hypoxic conditioning on arterial oxygen saturation," *Wilderness Environ. Med.*, vol. 20, no. 1, pp. 26–32, Mar. 2009, doi: 10.1580/08-WEME-OR-218.1.

[9] R. Jané, J. Lázaro, P. Ruiz, E. Gil, D. Navajas, R. Farré, and P. Laguna, "Obstructive sleep apnea in a rat model: Effects of anesthesia on autonomic evaluation from heart rate variability measures," in *Proc. CinC*, Zaragoza, Spain, vol. 40, 2013, pp. 1011–1014.

[10] I. Almendros, R. Farré, A. M. Planas, M. Torres, M. R. Bonsignore, D. Navajas, and J. M. Montserrat, "Tissue oxygenation in brain, muscle, and fat in a rat model of sleep apnea: Differential effect of obstructive apneas and intermittent hypoxia," *Sleep*, vol. 4, no. 8, pp. 1127–1133, Aug. 2011, doi: 10.5665/SLEEP.1176.

[11] R. Farré, M. Nacher, A. Serrano-Mollar, G. B. Galdiz, F. J. Alvarez, D. Navajas, and J. M. Monserrat, "Rat model of chronic recurrent airway obstructions to study the sleep apnea syndrome," *Sleep*, vol. 30, no. 7, pp. 930–933, Jul. 2007, doi: 10.1093/sleep/30.7.930.

[12] A. Navarrete-Opazo and G. S. Mitchell, "Therapeutic potential of intermittent hypoxia: A matter of dose," *Amer. J. Physiol.-Regulatory, Integrative Comparative Physiol.*, vol. 307, no. 10, pp. R1181–R1197, Nov. 2014, doi: 10.1152/ajpregu.00208.2014.

[13] A. Shimokawa, T. Kunitake, M. Takasaki, and H. Kannan, "Differential effects of anesthetics on sympathetic nerve activity and arterial baroreceptor reflex in chronically instrumented rats," *J. Auton. Nervous Syst.*, vol. 72, no. 1, pp. 46–54, Aug. 1998, doi: 10.1016/S0165-1838(98)00084-8.

[14] S. J. Kim, A. Y. Fong, P. M. Pilowsky, and S. B. G. Abbott, "Sympathoexcitation following intermittent hypoxia in rat is mediated by circulating angiotensin II acting at the carotid body and subfornical organ," *J. Physiol.*, vol. 596, no. 15, pp. 3217–3232, Aug. 2018, doi: 10.1113/JP275804.

[15] D. Romero and R. Jané, "Non-linear HRV analysis to quantify the effects of intermittent hypoxia using an OSA rat model," in *Proc. IEEE EMBC*, Berlin, Germany, Jul. 2019, pp. 4994–4997.

[16] R. Jane, P. Laguna, N. V. Thakor, and P. Caminal, "Adaptive baseline wander removal in the ECG: Comparative analysis with cubic spline technique," in *Proc. CinC*, Durham, NC, USA, 1992, pp. 143–147.
[17] J. P. Martinez, R. Almeida, S. Olmos, A. P. Rocha, and P. Laguna, "A wavelet-based ECG delineator: Evaluation on standard databases," *IEEE Trans. Biomed. Eng.*, vol. 51, no. 4, pp. 570–581, Apr. 2004, doi: 10.1109/TBME.2003.821031.
[18] A. J. Camm, M. Malik, J. T. Bigger, G. Breithardt, S. Cerutti, R. J. Cohen, and F. Lombardi, "Heart rate variability: Standards of measurement, physiological interpretation, and clinical use," *Circulation*, vol. 93, no. 5, pp. 1043–1065, 1996, doi: 10.1161/01.CIR.93.5.1043.
[19] J. Thireau, B. L. Zhang, D. Poisson, and D. Babuty, "Heart rate variability in mice: A theoretical and practical guide," *Exp. Physiol.*, vol. 93, no. 1, pp. 83–94, Jan. 2008, doi: 10.1113/expphysiol.2007.040733.
[20] G. J. J. Silva, M. R. Ushizima, P. S. Lessa, L. Cardoso, L. F. Drager, M. M. Atala, F. M. Consolim-Colombo, H. F. Lopes, I. A. Cestari, J. E. Krieger, and E. M. Krieger, "Critical analysis of autoregressive and fast Fourier transform markers of cardiovascular variability in rats and humans," *Brazilian J. Med. Biol. Res.*, vol. 42, no. 4, pp. 386–396, Apr. 2009, doi: 10.1590/S0100-879X2009000400012.
[21] L. E. V. Silva, V. R. Geraldini, B. P. de Oliveira, C. A. A. Silva, A. Porta, and R. Fazan, "Comparison between spectral analysis and symbolic dynamics for heart rate variability analysis in the rat," *Sci. Rep.*, vol. 7, no. 1, Aug. 2017, Art. no. 8428, doi: 10.1038/s41598-017-08888-w.
[22] N. Aimie-Salleh, M. Malarvili, and A. C. Phillip, "Quantitative comparison of time frequency distribution for heart rate variability using performance measure," *J. Wireless Commun. Netw.*, vol. 5, no. 2A, pp. 1–5, 2015. [Online]. Available: http://article.sapub.org/10.5923.c.jwnc.201501.01.html
[23] E. P. de Souza, M. A. Custaud, J. Frutoso, L. Somody, C. Gharib, and J. O. Fortrat, "Smoothed pseudo Wigner–Ville distribution as an alternative to Fourier transform in rats," *Auton. Neurosci.*, vol. 87, nos. 2–3, pp. 258–267, Mar. 2001, doi: 10.1016/S1566-0702(00)00211-3.
[24] F. Hlawatsch and G. F. Boudreaux-Bartels, "Linear and quadratic time-frequency signal representations," *IEEE Signal Process. Mag.*, vol. 9, no. 2, pp. 21–67, Apr. 1992, doi: 10.1109/79.127284.
[25] A. H. Costa and G. F. Boudreau-Bartels, "Design of time-frequency representations using a multiform, tiltable exponential kernel," *IEEE Trans. Signal Process.*, vol. 43, no. 10, pp. 2283–2301, Oct. 1995, doi: 10.1109/78.469860.
[26] M. Calvo, D. Romero, V. Le Rolle, N. Béhar, P. Gomis, P. Mabo, and A. I. Hernández, "Multivariate classification of brugada syndrome patients based on autonomic response to exercise testing," *PLoS ONE*, vol. 13, no. 5, May 2018, Art. no. e0197367.
[27] M. D. Costa, R. B. Davis, and A. L. Goldberger, "Heart rate fragmentation: A new approach to the analysis of cardiac interbeat interval dynamics," *Frontiers Physiol.*, vol. 8, p. 255, May 2017, doi: 10.3389/fphys.2017.00255.
[28] L. Pecchia, R. Castaldo, L. Montesinos, and P. Melillo, "Are ultra-short heart rate variability features good surrogates of short-term ones? State-of-the-art review and recommendations," *Healthcare Technol. Lett.*, vol. 5, no. 3, pp. 94–100, Jun. 2018, doi: 10.1049/htl.2017.0090.
[29] M. L. Munoz, A. van Roon, H. Riese, C. Thio, E. Oostenbroek, I. Westrik, E. J. C. de Geus, R. Gansevoort, J. Lefrandt, I. M. Nolte, and H. Snieder, "Validity of (ultra-)short recordings for heart rate variability measurements," *PLoS ONE*, vol. 10, no. 9, Sep. 2015, Art. no. e0138921, doi: 10.1371/journal.pone.0138921.
[30] F. Shaffer and J. P. Ginsberg, "An overview of heart rate variability metrics and norms," *Frontiers Public Health*, vol. 5, p. 258, Sep. 2017, doi: 10.3389/fpubh.2017.00258.
[31] I. Szollosi, H. Krum, D. Kaye, and M. T. Naughton, "Sleep apnea in heart failure increases heart rate variability and sympathetic dominance," *Sleep*, vol. 30, no. 11, pp. 1509–1514, Nov. 2007, doi: 10.1093/sleep/30.11.1509.
[32] C. Schlatzer, E. I. Schwarz, N. A. Sievi, C. F. Clarenbach, T. Gaisl, L. M. Haegeli, F. Duru, J. R. Stradling, and M. Kohler, "Intrathoracic pressure swings induced by simulated obstructive sleep apnoea promote arrhythmias in paroxysmal atrial fibrillation," *Europace*, vol. 18, no. 1, pp. 64–70, May 2015, doi: 10.1093/europace/euv122.
[33] R. Iturriaga, M. P. Oyarce, and A. C. R. Dias, "Role of carotid body in intermittent hypoxia-related hypertension," *Current Hypertension Rep.*, vol. 19, no. 5, p. 38, May 2017, doi: 10.1007/s11906-017-0735-0.
[34] L. T. Montemurro, J. S. Floras, P. Picton, T. Kasai, H. Alshaer, J. M. Gabriel, and T. D. Bradley, "Relationship of heart rate variability to sleepiness in patients with obstructive sleep apnea with and without heart failure," *J. Clin. Sleep Med.*, vol. 10, no. 3, pp. 271–276, Mar. 2014, doi: 10.5664/jcsm.3526.
[35] T. Shiomi, C. Guilleminault, R. Sasanabe, I. Hirota, M. Maekawa, and T. Kobayashi, "Augmented very low frequency component of heart rate variability during obstructive sleep apnea," *Sleep*, vol. 19, no. 5, pp. 370–377, Jul. 1996.
[36] J. Liang, X. Zhang, Y. Luo, T. Wang, L. Sun, and S. Huang, "The impact of respiratory events on the autonomic nervous system during sleep," *Int. Heart J.*, vol. 59, no. 2, pp. 378–386, Mar. 2018, doi: 10.1536/ihj.16-429.
[37] J. Liang, X. Zhang, X. He, L. Ling, C. Zeng, and Y. Luo, "The independent and combined effects of respiratory events and cortical arousals on the autonomic nervous system across sleep stages," *Sleep Breath*, vol. 22, no. 4, pp. 1161–1168, May 2018, doi: 10.1007/s11325-018-1669-8.
[38] A. Shimokawa, T. Kunitake, M. Takasaki, and H. Kannan, "Differential effects of anesthetics on sympathetic nerve activity and arterial baroreceptor reflex in chronically instrumented rats," *J. Autonomic Nervous Syst.*, vol. 72, no. 1, pp. 46–54, Aug. 1998, doi: 10.1016/S0165-1838(98)00084-8.

DANIEL ROMERO received the M.S. degree in telecommunications engineering from the University of Orient, Cuba, and the Ph.D. degree in biomedical engineering from the University of Zaragoza, Spain, in 2004 and 2013, respectively.

From 2004 to 2007, he was an Assistant Professor with the Department of Telecommunications, University of Oriente, and a Postdoctoral Researcher with the Signal and Image Processing Laboratory (LTSI-INSERM), Rennes, France, from 2014 to 2018. Since 2018, he has been a Postdoctoral Researcher with the Institute for Bioengineering of Catalonia (IBEC), Barcelona, Spain. His current research interests are focused on the development of advanced signal processing techniques and data-driven models, combined with machine learning techniques and Big–Data analytic focused on biomedical applications, to improve the diagnosis and prognosis of cardiovascular and respiratory diseases.

RAIMON JANÉ (Senior Member, IEEE) received the Ph.D. degree from the Universitat Politècnica de Catalunya (UPC), Barcelona, Spain, in 1989.

Since 2008, he has been the Principal Investigator of the Biomedical Signals and Systems (SISBIO) Group and a member of the Steering Committee of the Centro de Investigación Biomédica en Red de Bioingeniería, Biomateriales y Nanomedicina (CIBER–BBN). He is currently the Director of Research with the Department of Automatic Control (ESAII), UPC, and the Scientific Group Leader of the Biomedical Signal Processing and Interpretation Group, Institute for Bioengineering of Catalonia (IBEC), Barcelona Institute of Science and Technology (BIST), Barcelona. He is also a Professor in the master's degree program and is the Coordinator of the Ph.D. program in biomedical engineering. His research interests include multimodal and multiscale biomedical signal processing in cardiorespiratory diseases and sleep disorders.

Dr. Jané is currently a member of the IEEE EMBS Technical Committee on Cardiopulmonary Systems. In 2005, he received the Barcelona City Prize from the Barcelona City Council for technology research. He is an Associate Editor of the *Cardiovascular and Respiratory Systems Engineering Theme* of the IEEE EMBC. He was the President of the Spanish Society of Biomedical Engineering (SEIB), from 2012 to 2020.